Identifying Uncertainty in Laser Powder Bed Fusion Additive Manufacturing Models

Felipe Lopez[1]
Department of Mechanical Engineering,
University of Texas at Austin,
Austin, TX 78712
e-mail: felipelopez@utexas.edu

Paul Witherell
Systems Integration Division,
National Institute of Standards and Technology,
Gaithersburg, MD 20899

Brandon Lane
Intelligent Systems Division,
National Institute of Standards and Technology,
Gaithersburg, MD 20899

As additive manufacturing (AM) matures, models are beginning to take a more prominent stage in design and process planning. A limitation frequently encountered in AM models is a lack of indication about their precision and accuracy. Often overlooked, model uncertainty is required for validation of AM models, qualification of AM-produced parts, and uncertainty management. This paper presents a discussion on the origin and propagation of uncertainty in laser powder bed fusion (L-PBF) models. Four sources of uncertainty are identified: modeling assumptions, unknown simulation parameters, numerical approximations, and measurement error in calibration data. Techniques to quantify uncertainty in each source are presented briefly, along with estimation algorithms to diminish prediction uncertainty with the incorporation of online measurements. The methods are illustrated with a case study based on a thermal model designed for melt pool width predictions. Model uncertainty is quantified for single track experiments, and the effect of online estimation in overhanging structures is studied via simulation.
[DOI: 10.1115/1.4034103]

1 Introduction

AM is the use of layer-based processes for producing parts directly from computer models, without part-specific tooling [1]. Since its introduction in the mid-1980 s, AM has become popular because of its ability to produce complex geometries that were impossible with traditional manufacturing techniques. Despite growing popularity, AM technologies still present some unresolved challenges that hinder their widespread adoption. Among these challenges are high process variability, unsatisfactory part quality, and lack of standards; all of which originate from the limited knowledge of this relatively new set of processes. Many have looked toward modeling to achieve a deeper understanding of the physics of AM processes and to assist in the qualification of AM-produced components, which currently relies exclusively on experiments. Although most models published in the literature have been compared with experimental measurements, they often ignore process variability and lack measures of the precision and accuracy of their deterministic predictions. Some of the few examples of uncertainty quantification (UQ) in AM models can be found in the papers by Moser et al. [2] and Ma et al. [3], both of which studied model sensitivity to uncertainty in input parameters; and Kamath [4], who discussed uncertainty in data-driven surrogate models.

In general, knowledge of uncertainty in AM models is required for: (a) model validation, which compares simulation results and experimental data accounting for uncertainty in both sources; (b) decision-making, where model predictions and their probabilities may be used to make informed decisions, such as the qualification and certification of designs and manufacturing plans; and (c) uncertainty management, to identify the sources with the largest relative contributions to the overall prediction error.

Model-based qualification in the specific case of L-PBF will require control of several qualities, such as reduction of over- and undermelting defects, desired microstructure and mechanical properties, and reduction of residual stresses. In this paper, we use melt pool dimensions as key performance indicators (KPIs) due to their direct relationship with the thermal processes that define such qualities [5]. Out of the set of melt pool dimensions, melt pool width is chosen as the primary KPI because it can be traced both during and after the build. Other approaches, intended only for preprocess optimization, may focus on different KPIs (e.g., cross-sectional area and length-to-depth ratio) [6].

This paper provides: (a) a discussion on methods for UQ in L-PBF models; (b) an example of UQ in which all the sources of error are considered; and (c) a method for quantifying unmodeled process perturbations with potential applications in feedback control.

2 Identifying Uncertainty in L-PBF Models

In engineering, computational models are designed as approximations of physical reality and, as such, are subjected to a cascade of errors and uncertainties. Figure 1 illustrates recognized sources of modeling errors [7], which we have adapted for an AM application. Four sources of uncertainty can be observed: modeling errors, errors in simulation inputs, numerical errors, and measurement errors.

L-PBF involves multiple physical phenomena occurring at different times and length scales. Due to the complexity of the process, most computational models limit their scope to a subset

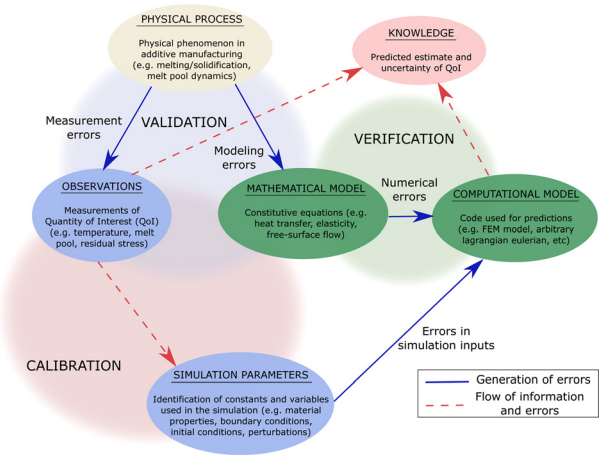

Fig. 1 Cascade of sources of error in computer models of AM

[1]Corresponding author.

Contributed by the Design Automation Committee of ASME for publication in the JOURNAL OF MECHANICAL DESIGN. Manuscript received March 28, 2016; final manuscript received July 6, 2016; published online September 12, 2016. Assoc. Editor: Samy Missoum.

of physical phenomena at a given scale, neglecting dynamics not captured by them and introducing modeling uncertainty. Some common sources of modeling uncertainty in L-PBF can be found in: (a) particle-level dynamics neglected in continuum models [8,9], (b) inaccurate distributions for laser power acting on the powder bed, or (c) an inadequate choice of boundary conditions that neglects track-to-track and layer-to-layer interactions [3,5,10].

Input uncertainty is the result of inaccurate simulation parameters, adopted in lieu of more precise knowledge or as result of uncertainty in the training data. In the case of L-PBF models, common sources can be found in: (a) absorption coefficient, which quantifies the amount of irradiated laser power that heats up the powder bed [11]; (b) thermal conductivity in loose powder, which depends on the distribution of powder particles [3]; (c) thermophysical parameters at high temperatures [10]; (d) convection and radiation coefficients [10]; and (e) enhancing coefficients occasionally used to account for the effect of advection in the liquid [12].

Commercial modeling packages, mostly based on finite element methods, are often the preferred tools to solve AM mathematical models, but other methods (e.g., discrete element methods and lattice Boltzmann methods) are rapidly capturing the attention of the AM community. Commercial packages used for L-PBF models often include convergence studies to ensure that numerical error is small, but its magnitude is seldom reported.

Measurement uncertainty depends solely on the methods and instruments used to gather test data. The choice of appropriate measurement techniques for L-PBF is an unsolved issue, and it depends on the KPI of interest [13].

3 UQ

A comprehensive discussion on uncertainty sources in heat transfer and fluid mechanics models can be found in the standard ASME V&V 20 [14]. The fact that AM involves thermally activated consolidation processes makes this standard suitable for this application. Figure 2 illustrates the process of prediction and validation followed in UQ with ASME V&V 20. The process starts with a known set of processing parameters and material properties, which are fed to the model to obtain a simulation result S. Information about the grid is used to estimate the numerical error δ_{num} that results from the numerical method. Meanwhile, an assumed probability distribution of simulation parameters is propagated through the model to estimate the error due to inaccurate inputs δ_{input}. Finally, simulation results S are confronted with measurements D and measurement error δ_D. The difference between model prediction and measurement determines the bias E, which acts as an estimate of modeling error δ_{model}. All the sources of error are merged in the calculation of prediction uncertainty, which is reported along with the bias.

Process variability in AM models is accounted for as uncertainty due to unknown inputs, if it can be traced back to simulation parameters, or as modeling uncertainty otherwise. Herein, we describe an application of Bayesian estimation to reduce modeling error by mapping sources of variability to random simulation parameters that are identified in real time. In the case of L-PBF, the set of identified parameters may include random variables that attempt to model the variable thermal characteristics of the material that surrounds the melt pool.

The process for online estimation is illustrated in Fig. 3. In this case, a simulation is performed for a given set of parameters and an initial state with its associated uncertainty, which originate from a previous simulation. The propagated state and process uncertainty (modeling, numerical, and input) are then compared with the measurement and its uncertainty to obtain estimates of the state at the next time-step, its uncertainty, and an updated estimate of process uncertainty.

4 Case Study: Uncertainty in a Stochastic Model for L-PBF AM

In this section, we present a case study describing how different sources of uncertainty can be identified and subsequently incorporated into a predictive model. We choose a thermal model developed for laser cladding [15] but adjusted for use in L-PBF. The model provides a set of ordinary differential equations (ODEs) that describe the motion of isotherms on the surface of the powder bed. If one of these isotherms is assigned to the melting temperature, the model can be used to dynamically track the location of the solidification front and predict melt pool width.

The set of ODEs is modified with the inclusion of diffusion efficiency (μ), a random variable that multiplies thermal diffusivity and is used to correct for variable sideways thermal diffusion due to unmodeled process perturbations. Its value is set to one in nominal cases, when the melt pool is surrounded by fully dense material. In the case of overhanging structures, for example, a decrease of thermal diffusivity toward the bottom improves heat transfer to the sides, increasing the value of μ.

The proposed model is fast, returning a melt pool width prediction in 0.1 s when solved with MATLAB R2014b's ode23 function running on an Intel Core i7-3770 CPU.

4.1 UQ. Uncertainty is quantified by comparing simulation results for fully dense material ($\mu = 1$) with melt pool width measurements gathered from an alloy 625 plate, as described by Montgomery et al. [16]. Single bead tests were performed using different combinations of laser power and scan speed. In this study, error is approximated within the interval $\delta_{\text{model}} \in [E - u_{\text{val}}, E + u_{\text{val}}]$ centered around $E = S - D$. Validation uncertainty u_{val}, which accounts for uncertainty from all the sources, can be computed following $u_{\text{val}} = \sqrt{u_{\text{num}}^2 + u_{\text{input}}^2 + u_D^2}$ under the assumption that all the error sources are independent.

The first steps toward quantification of modeling error are code and solution verification. Code was verified with a manufactured solution and it was observed that the method converges to analytical solutions for constant material properties and infinitely fine

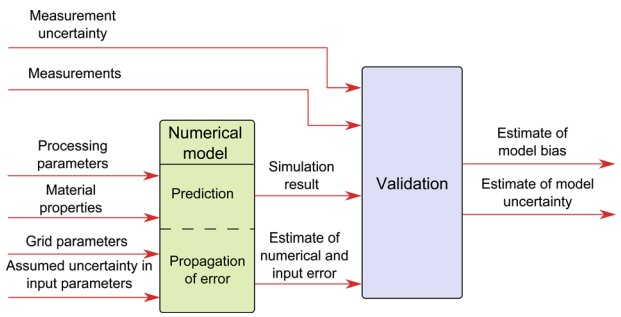

Fig. 2 V&V and UQ in computational models as suggested in ASME V&V 20

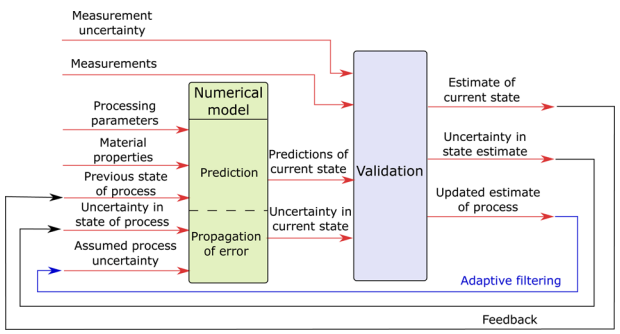

Fig. 3 Online estimation in predictive models

Table 1 Assumed distributions for normally distributed input parameters

Input	Nominal	Standard deviation (% nominal)
Power	195 W	2.5%
Speed	0.800 m/s	1.5%
Absorption coefficient	0.6	25%
Latent heat	2.97×10^5 J/kg	5.0%
Melting temperature	1320 °C	5.0%
Thermal diffusivity	Function of T_i	10.0%

grid. Similar convergence studies were performed for predictions of melt pool width using temperature-dependent material properties. Successive grid refinement was used to identify an order of accuracy of $p = 1.9$, which was lower than the formal order of accuracy ($p = 3$), presumably due to the effect of nonlinearities in the temperature-dependent properties. Numerical uncertainty was quantified using Roache's grid convergence index [14] for a grid of ten isotherms. The numerical prediction for melt pool width for 195 W and 800 mm/s was found at (127.3 ± 2.7) μm ($\pm 2.12\%$).

The second source of uncertainty comes from imperfect knowledge of input parameters. Six factors were selected for a Monte Carlo study to determine the propagation of uncertainty in inputs: laser power, scan speed, absorption coefficient, latent heat, melting temperature, and thermal diffusivity. All the factors were assumed to be normally distributed and are given in Table 1. Nominal values for temperature-dependent material properties were obtained from the TCN16 thermodynamic database [17], while nominal absorptivity was identified experimentally. The variability assumed for most input parameters was based on the work of Ma et al. [3], except for that of absorptivity which was enhanced. A Monte Carlo approximation of the probability distribution of melt pool width was obtained for 4000 samples. The result had a normal distribution and a 95% confidence interval found in (131.6 ± 37.3) μm.

The last source of uncertainty comes from validation experiments performed with a Zeiss AxioVision AX10 optical microscope. Each image was measured 15 times along the width at approximately equal spacing. Results were averaged and showed a standard deviation of 5.2 μm, suggesting a ± 10.4 μm confidence interval.

Measured melt pool widths were compared to predictions obtained from the model, only for data points close to nominal operating conditions (195 W and 800 mm/s). The region of calibration for this model was delimited between 150 W and 195 W, and 600 mm/s and 1000 mm/s. Assuming that all the error sources are independent, validation uncertainty was estimated at (127.3 ± 38.8) μm ($\pm 30.5\%$) for nominal operating conditions.

It can be observed that modeling uncertainty is relatively large, as expected due to the simplification of the thermal problem by assuming a point source instead of a distributed one. The absence of other physical phenomena considered important for melt pool dynamics, such as surface tension, also contributes to modeling error. Numerical uncertainty, however, was negligible even for a coarse grid. On the other hand, input parameters have a significant contribution to model uncertainty, partially due to the large uncertainty assumed for the absorption coefficient. Extrapolation of the modeling error to the other points in the region of calibration matched the obtained measurements, as observed in Fig. 4.

The relatively large prediction uncertainty is compensated by the speed of the model. The model, in its current form, can be used as a first step toward process planning by providing users with computationally inexpensive predictions to explore the effects of laser power and speed in melt pool geometry.

4.2 Bayesian Estimation. Diffusion efficiency may be allowed to vary in time to account for unmodeled track-to-track and layer-to-layer interactions. In this section, we present an

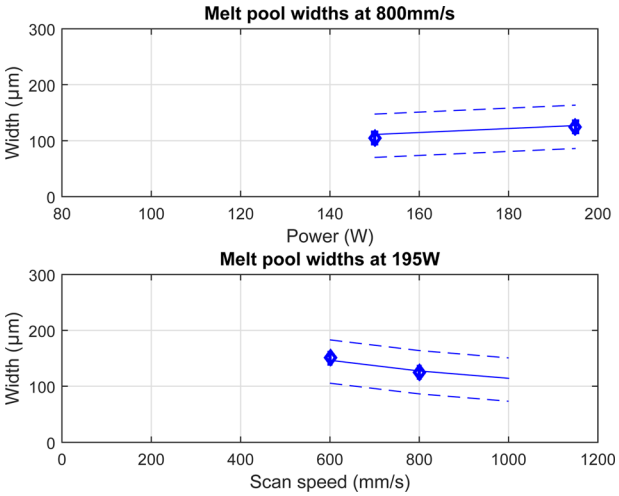

Fig. 4 Melt pool width predictions (continuous line) and measurements (points) for single track scans with alloy 625

example that illustrates how online thermographic monitoring could potentially be used to identify unmodeled dynamics and decrease uncertainty in melt pool width predictions. The case study is designed to represent a horizontal overhanging plane which is scanned in a direction perpendicular to the solid-to-powder transitions. This case study, designed and published by Kruth et al. [5], showed that melt pool area increases threefold when going through this kind of overhangs. Synthetic data were generated to mimic this event by artificially perturbing μ and assuming that it varies instantaneously from 1 to 2.2 when melting on top of loose powder. In this study, it has been assumed that the isotherms between 576 °C and 1072 °C can be detected with thermographic sensors. To simulate measurement uncertainty, noise was added to the measured isotherm widths following a standard deviation of 26 μm, which corresponds to half the pixel width in a similar thermographic setting.

Process estimation, using a linear stochastic version of the model and a Kalman filter [18], results in the estimates shown in Fig. 5, where the null hypothesis of normal operation (no

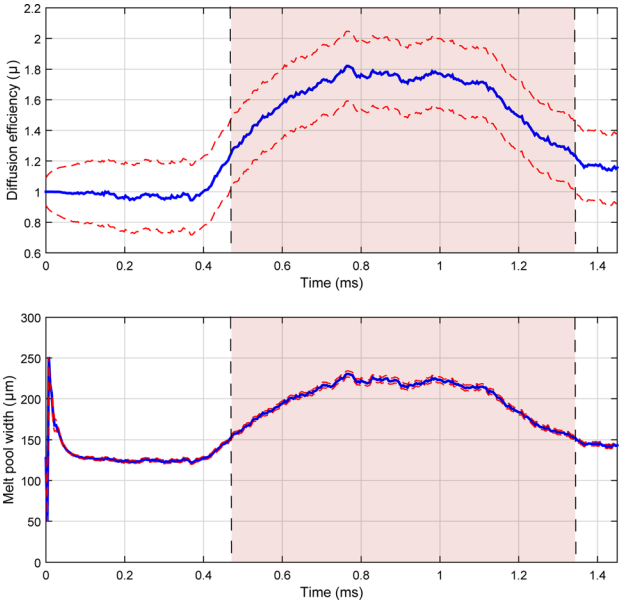

Fig. 5 Estimated diffusion efficiency and melt pool width. Predictions are plotted as continuous lines and 95% confidence intervals are given in dashed lines.

overhang, $H_0 : \mu = 1$) is rejected in favor of the alternative hypothesis of an anomaly ($H_A : \mu \neq 1$) in the shaded region. Response speed and accuracy and uncertainty in the estimates are expected to be dependent on the process and measurement uncertainty used for estimation, which were assumed in this example and will have to be adjusted in an experimental study.

An important point to be observed is the low uncertainty in the melt pool width prediction even in the region of anomalous operation. Without online measurements, models would have to account for the potential variation in diffusion efficiency using large uncertainties for μ, and increasing uncertainty in melt pool width predictions. For example, if the study to determine sensitivity to input parameters is repeated letting μ vary following $\mu \sim \text{Unif}[1.0, 2.5]$, the obtained prediction is (193.6 ± 106.6) μm ($\pm 55.1\%$), which is much wider than the confidence intervals reported in Fig. 5 (± 4.0 μm).

5 Conclusions

As metal-based AM gains popularity, closer attention has been paid to the computational models developed to predict quality in manufactured components. Such predictions could be used to aid design and process planning by allowing engineers to make adjustments for improved quality. One aspect that has been traditionally ignored in these models is that, if they are to be used in model validation or for certification of parts, one must know how accurate these models are. UQ presents a set of challenges that have often been ignored both by manufacturing and modeling engineers.

A method to decrease modeling error, by mapping it to random simulation inputs that are identified in real time, is illustrated. Inclusion of random inputs requires that the assumed randomness is validated and adjusted, which can be done with adaptive filtering. The proposed estimation method could potentially be used for real-time control to maintain desired melt pool geometries in L-PBF even when process perturbations are detected.

Though the case study presented in this paper is based on a low-order model, the same ideas can be extended to high-order models. The algorithms used for UQ, however, are different. For instance, the high computational cost of Monte Carlo methods prevents their application in the propagation of uncertainty in input parameters.

Acknowledgment

Official contribution of the National Institute of Standards and Technology (NIST); not subject to copyright in the United States. The full descriptions of the procedures used in this paper may require the identification of certain commercial products. The inclusion of such information should in no way be construed as indicating that such products are endorsed by NIST or are recommended by NIST or that they are necessarily the best materials, instruments, software, or suppliers for described purposes.

References

[1] Bourell, D., Beaman, J., Marcus, H., and Barlow, J., 1990, "Solid Freeform Fabrication: An Advanced Manufacturing Approach," International Solid Freeform Fabrication Symposium, pp. 1–7.
[2] Moser, D., Beaman, J., Fish, S., and Murthy, J., 2014, "Multi-Layer Computational Modeling of Selective Laser Sintering Processes," ASME Paper No. IMECE2014-37535.
[3] Ma, L., Fong, J., Lane, B., Moylan, S., Filliben, J., Heckert, A., and Levine, L., 2015, "Using Design of Experiments in Finite Element Modeling to Identify Critical Variables for Laser Powder Bed Fusion," International Solid Freeform Fabrication Symposium, pp. 219–228.
[4] Kamath, C., 2016, "Data Mining and Statistical Inference in Selective Laser Melting," Int. J. Adv. Manuf. Technol., published online.
[5] Kruth, J.-P., Mercelis, P., Van Vaerenbergh, J., and Craeghs, T., 2007, "Feedback Control of Selective Laser Melting," 3rd International Conference on Advanced Research in Virtual and Rapid Prototyping, Leiria, Portugal, Sept. 24–29, pp. 521–527.
[6] Gockel, J., Beuth, J., and Taminger, K., 2014, "Integrated Control of Solidification Microstructure and Melt Pool Dimensions in Electron Beam Wire Feed Additive Manufacturing of Ti-6Al-4V," Addit. Manuf., **1–4**, pp. 119–126.
[7] Oden, T., Moser, R., and Ghattas, O., 2010, "Computer Predictions With Quantified Uncertainty—Part I," SIAM News, **43**(9), p. 1842.
[8] Khairallah, S. A., Anderson, A. T., Rubenchik, A., and King, W. E., 2016, "Laser Powder-Bed Fusion Additive Manufacturing: Physics of Complex Melt Flow and Formation Mechanisms of Pores, Spatter, and Denudation Zones," Acta Mater., **108**, pp. 36–45.
[9] Riedlbauer, D., Scharowsky, T., Singer, R. F., Steinmann, P., Körner, C., and Mergheim, J., 2016, "Macroscopic Simulation and Experimental Measurement of Melt Pool Characteristics in Selective Electron Beam Melting of Ti-6Al-4V," Int. J. Adv. Manuf. Technol., published online.
[10] Roberts, I. A., 2012, "Investigation of Residual Stresses in the Laser Melting of Metal Powders in Additive Layer Manufacturing," Ph.D. thesis, University of Wolverhampton, Wolverhampton, UK.
[11] Moser, D., Pannala, S., and Murthy, J., 2015, "Computation of Effective Radiative Properties of Powders for Selective Laser Sintering Simulations," JOM, **67**(5), pp. 1194–1202.
[12] Cheng, B., Price, S., Lydon, J., Cooper, K., and Chou, K., 2014, "On Process Temperature in Powder-Bed Electron Beam Additive Manufacturing: Model Development and Validation," ASME J. Manuf. Sci. Eng., **136**(6), p. 061018.
[13] Mani, M., Lane, B., Donmez, A., Feng, S., Moylan, S., and Fesperman, R., 2015, "Measurement Science Needs for Real-Time Control of Additive Manufacturing Powder Bed Fusion Processes," National Institute of Standards and Technology, Gaithersburg, MD, Standard No. NISTIR 8036.
[14] ASME, 2009, "Standard for Verification and Validation in Computational Fluid Dynamics and Heat Transfer," American Society of Mechanical Engineers, New York, Standard No. ASME V&V 20-2009.
[15] Devesse, W., De Baere, D., and Guillaume, P., 2014, "The Isotherm Migration Method in Spherical Coordinates With a Moving Heat Source," Int. J. Heat Mass Transfer, **75**, pp. 726–735.
[16] Montgomery, C., Beuth, J., Sheridan, L., and Klingbeil, N., 2015, "Process Mapping of Inconel 625 in Laser Powder Bed Additive Manufacturing," Solid Freeform Fabrication Symposium, pp. 1195–1204.
[17] Thermo-Calc, 2014, THERMO-CALC AB VERSION 3.1, Thermo-Calc, Stockholm, Sweden.
[18] Kalman, R. E., 1960, "A New Approach to Linear Filtering and Prediction Problems," ASME J. Basic Eng., **82**(1), pp. 35–45.